Denoised CT Images Quality Assessment Through COVID-19 Pneumonia Detection Task

Lumi Xia, Houda Jebbari, Lucie Lévêque, Olivier Deforges, Meriem Outtas, Lu Zhang

Denoised CT Images Quality Assessment Through COVID-19 Pneumonia Detection Task

Lumi Xia, Houda Jebbari, Olivier Deforges, Lu Zhang, Meriem Outtas
INSA Rennes
CNRS
IETR, UMR 6164
Rennes, France
Firstname.Lastname@insa-rennes.fr

Lucie Lévêque
École Centrale Nantes
LS2N, UMR 6004
Nantes Université
Nantes, France
lucie.leveque@univ-nantes.fr

***Abstract*—Medical images largely contribute to the diagnosis of lung diseases, especially pneumonia, an inflammation of lungs tissue. Since the emergence of COVID-19 in late 2019, medical imaging systems, notably computed tomography (CT) scans, have considerably helped in its diagnosis as well as revealing its infection severity. Serving as such an important role in clinical practice, the quality of medical images is therefore crucial for an accurate diagnosis. Denoising techniques, as a common image processing method, are being more and more used in medical imaging. However, how image denoising technique influences medical images' quality in terms of diagnostic performance still remains to be answered. In this paper, a primary study was carried out thanks to a detection task-based image quality assessment experiment, where we explored the performance of COVID-19 classifiers on both original and denoised chest CT scans. Two different denoising methods, i.e., anisotropic diffusion (AD) and total variation (TV) filters, were used. Results showed that the TV denoised model performed better than both baseline and AD denoised model, despite its less favorable mathematical image quality metrics.**

***Index Terms*—COVID-19 classification, image quality assessment, task-based quality, computed tomography, image denoising**

I. Introduction

SINCE December 2019, COVID-19 has caused a worldwide severe health crisis . The reverse transcription polymerase chain reaction (RT-PCR) test has been widely used to diagnose this disease from the beginning of the pandemic. This method is effective to detect the presence of the virus; however, it does not allow a clear diagnosis on the disease's severity. To address this limitation, and as the COVID-19 mainly affects lungs, physicians used computed tomography (CT) scans to visualise lung damage, as well as the spread of the infection [1]. Indeed, lung infection by COVID-19 presents distinct characteristics; the most common CT patterns are ground glass opacities (GGOs) and consolidations, related to the stage and severity of the disease [2]. Comparing to RT-PCR test, the main advantages of CT imaging encompass its accuracy and low scanning time [3]. Consequently, with the number of COVID-19 cases exponentially increasing, health professionals have been using CT scans for rapid identification and isolation of infected individuals, or even for an early prevention of the disease. Moreover, the comparisons between CT scans and RT-PCR test results of COVID-19 patients at early stages showed that abnormalities on the CT images may appear before RT-PCR positivity [4].

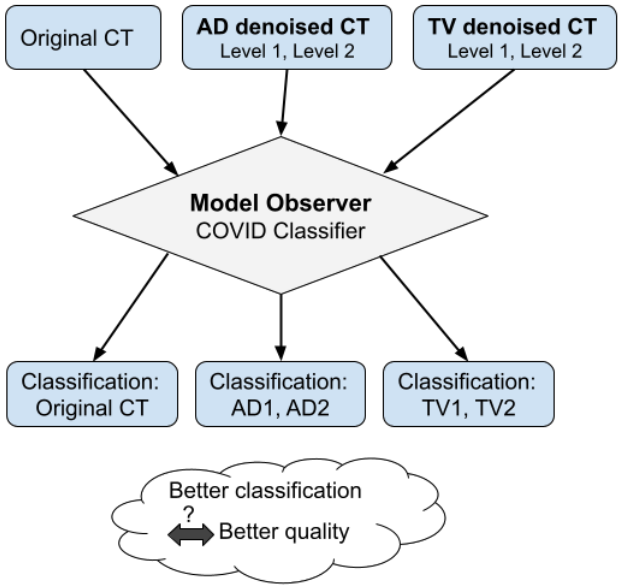

Fig. 1. Protocol to evaluate the quality of COVID-19 CT images with an objective task-based approach.

Despite all these advantages, CT scans are realized by a series of X-ray beams, inevitably generating radiation risk for patients, which, in some cases, causes cancer [5]. A solution to lessen this issue is to reduce the radiation dose, at the cost of more noise and artifacts related to the reduced dose. Some other factors during image acquisition, transmission, and reconstruction also contribute to the noise in medical images [6]. However, adequate image quality, which provides enough and reliable diagnostic information for doctors, is crucial in clinical practice. To achieve better image quality, denoising methods are commonly employed in image processing, including in the medical imaging domain [7]. Meanwhile, the influence of image denoising techniques on medical image quality is not

yet well studied. Besides, unlike for natural images, where there are numerous image quality assessment (IQA) metrics [8], [9], standards developed specially for medical image quality assessment are still under discussion. Some other IQA methods therefore need to be explored to evaluate medical images quality.

As good medical image quality insures and increases confidence of decisions in a diagnostic task, it can be defined as how well desired information can be extracted from an image, or the performance of an observer for a given task [10]. In the literature, several studies have intended to assess the performance of medical experts using this so-called *task-based approach* for lesion detection or localisation [11]. Even though radiologists are considered the gold standard for medical IQA, subjective experiments are time-consuming and tedious. There is therefore a great need for model observers (MOs), i.e., numerical models that can perform the same tasks as humans [12]. To perform an efficient task-based assessment, several elements have to be defined, i.e., population, observer, task, and figure of merit (FOM), to assess how observers perform [13]. The detection task is the most commonly addressed task by traditional MOs, which are mainly based on mathematical methods [12]. Some widely known models are as follows: ideal observer (IO), formulated in terms of Bayesian statistical inference [14]; hotelling observer (HO), a practical alternative to the IO using a linear discriminant [10]; and channelised hotelling observer (CHO), that approximates the HO using effective channels or a series of filters [15]. Artificial intelligence (AI)-based MOs have been recently undergoing a significant evolution, whereas traditional MOs need a huge amount of computation and data. Like traditional models, they aim to approximate the statistical test by training a model to maximise a specific FOM, or solving an optimisation problem. Few studies [16], [17] proposed supervised learning-based approaches and demonstrated good accuracy and sensitivity in detecting anomalies. Zhou *et al.* presented a study using deep learning (DL) methods for binary signal detection tasks [18]. They employed artificial neural networks to approximate the IO and HO, by a convolutional neural network (CNN) and a single layer neural network (SLNN), respectively. The performance of developed observers were compared to traditional observers in terms of computational feasibility. The authors succeeded in approximating traditional MOs with good accuracy on computer-simulated images.

Ideally, in the medical context, denoising methods shall remove noise while preserving clinical information [19]. Several studies presented very interesting works on low-dose CT denoising using deep learning, such as the sharpness-aware low-dose CT denoising generative adversarial network (SAGAN) [20], the radiologist-inspired deep neural network (RIDnet) [21], and the generative adversarial network with Wasserstein distance and perceptual loss (WGAN-VGG) [22]. Li *et al.* proposed denoising methods based on deep neural networks on synthetic medical images and evaluated the image quality using task-based approach, on simulated images, and concluded on *loss of task-relevant information* [23].

The purpose of our study is to assess, using an objective task-based method, the quality of real (i.e., non-simulated) CT images on the COVID-19 pneumonia detection task. More specifically, we applied two commonly used denoising methods, the anisotropic diffusion (AD) and total variation (TV) filters, on a publicly available COVID-19 dataset of chest CT scans, to generate denoised CT images, then evaluated the quality of these images along with the original ones by a COVID-19 classifier, as illustrated in Figure 1.

II. Method

As mentioned previously, CT scans have been used to help with the diagnosis, prognosis, and monitoring of COVID-19, and thus provide a large source of data for scientific studies. The objective of our research is the evaluation of CT image quality for the detection of COVID-19 using a task-based approach. For this goal, we decided to apply a COVID-19 classifier to achieve the detection task, rather than approximating traditional MOs using AI. Hence, a present *vs.* absent signal / COVID classification gives out the medical image quality evaluation. This detection task is applied on both the original images and the denoised ones, enabling to figure out the effect of denoising methods and levels on CT image quality.

A. COVID-19 database

Compared to the huge selection of natural image databases, medical imaging databases suffer from a lack of content and from the unavailability of large amounts of labeled experimental data [24].

The dataset selection criteria for our study were as follows. It should contain 1) both COVID-19 and non-COVID-19 cases, 2) chest CT scans, 3) a wide variety of data with many well-labeled training cases, and 4) the dataset should have been collected from single equipment and reconstruction algorithms. Therefore, the COVID-CT-MD dataset [25] was chosen, which contains 171 COVID-19 cases, 76 healthy cases, as well as 60 community-acquired pneumonia (CAP) cases. It has further been reviewed and annotated by radiologists.

For our study, we selected 36 COVID-19 infected patients, as well as 36 healthy cases, with detailed labels for this experiment. To be more specific, 183 COVID slices and 191 non-COVID slices from those patients were chosen as training dataset, while the validation dataset consisted of 86 COVID slices 89 non-COVID slices.

B. COVID-19 classifier

Extensive research has been carried out on the application of signal processing and AI in COVID-19 classification. These COVID-19 classifiers can be divided into three categories: 1) DL models developed from scratch [26], 2) transfer learning on pre-trained DL models [27], [28], and 3) machine learning (ML) models on extracted features [29], [30]. Some classifiers combined both DL and ML techniques, by employing DL networks as feature extractors [31].

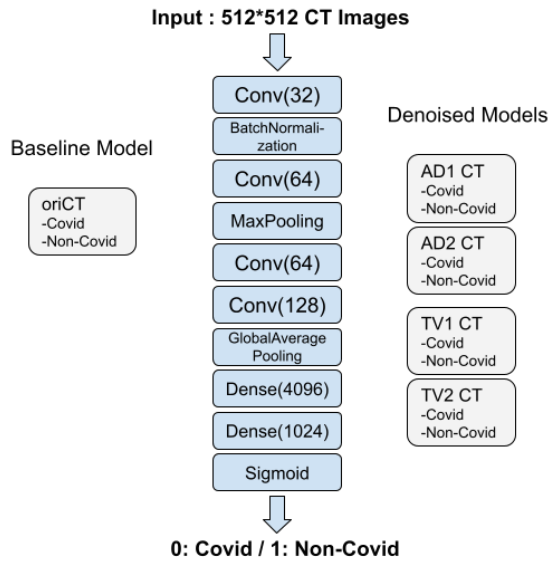

Fig. 2. Architecture of proposed COVID-19 classifier

In this study, we firstly tested the COVID-FACT[1] classifier [32] accompanied with the chosen database, i.e., COVID-CT-MD. It reached an accuracy of 0.92. The COVID-FACT classifier is a fully automated network for identifying COVID-19 cases from capsule network-based chest CT scans. The model processes in three steps, i.e., lung segmentation, selection of infected slices, and classification of cases as COVID-19 vs. non-COVID-19.

Since our goal here was the COVID-19 classification, we developed a simpler but more efficient CNN model, with less computing complexity and higher accuracy. The architecture of this classifier is shown in Figure 2. It mainly consists of four convolutional layers, one max pooling layer, one global average pooling layer, and three fully connected layers. The input is CT images at their original size 512*512, and the output is a probability between 0 (referring to COVID-19) and 1 (referring to non-COVID-19).

Training parameters were set as follows: Adam optimiser with learning rate at $1e^{-4}$, loss function as binary cross entropy, batch size at 4, and epochs at 100.

C. Denoising methods

Whether denoising methods can improve the performance of model observers on COVID-19 pneumonia detection tasks remains unexplored. We therefore applied two traditional denoising methods on the COVID-CT-MD database, i.e., the anisotropic diffusion (AD) filter [33] and the total variation (TV) filter [34]. The choice of these filters was made based on a review on CT image noise and its denoising methods [7].

First brought up by Perona and Malik [35], AD filtering is used to remove noises without losing image edges. Its principle is to generate a series of successively more and more blurred images from one image, based on a diffusion process, as described in Equation 1:

$$\begin{aligned} I_n &= div(c(x,y,n)\nabla I) \\ c(x,y,n) &= g(\nabla I) = e^{(-\frac{||\nabla I||}{K})^2} \end{aligned} \tag{1}$$

where I_n is the blurred image of input image I after nth iteration; ∇ is the gradient operator; constant $c(x,y,n)$ is the diffusion rate, whose value is a function of $||\nabla I||$; constant K controls the sensitivity to edges, which is usually determined beforehand or as a function of image noise.

TV filtering aims to reduce the total variation of an image, which reflects the noise level, while maximally preserving the details of original image [36]. Mathematically, this process is defined by Equation 2 as follows:

$$\begin{aligned} V(I) &= \sum_{i,j}(\sqrt{|I_{i+1,j} - I_{i,j}|^2} + \sqrt{|I_{i,j+1} - I_{i,j}|^2}) \\ \min_I &= E(I_0, I) + \lambda V(I) \end{aligned} \tag{2}$$

where $V(I)$ is the total variation of an image; $E(I_0, I)$ is the 2D L_2 norm of original image I_0 and denoised image, which is found by minimizing this second equation; constant λ is the denoising weight, and the larger λ leads to more blurred denoised image.

In our experiments, we applied these two denoising methods with two different sets of parameters, as shown in Table I, in order to explore the influence of different denoising levels. These four datasets (i.e., AD1, AD2, TV1, TV2) generated from original CT dataset were used for training our COVID classifier.

TABLE I
DENOISING METHODS PARAMETERS

Denoised Image	Parameters
AD1	$K = 10, n = 10$
AD2	$K = 50, n = 50$
TV1	$\lambda = 0.0001$
TV2	$\lambda = 0.1$

III. RESULTS

A. Denoised CTs

With the methods mentioned in section II-C, we generated four denoised datasets. Figure 3 presents an example of these datasets, where the first row represents the original CT image (oriCT) and four denoised images; the second row displays the region of interest (ROI), that is to say the COVID lesion in corresponding images; and the last row demonstrates the difference between every denoised image and oriCT, i.e., the noise image that subtracted from oriCT.

As shown in Figure III-A, all these four denoised images are more blurry comparing to the original one, especially AD2 ad TV2, where the denoising level is higher. We can also see from Figure III-A that both denoising methods have different denoising patterns.

[1]https://github.com/ShahinSHH/COVID-FACT

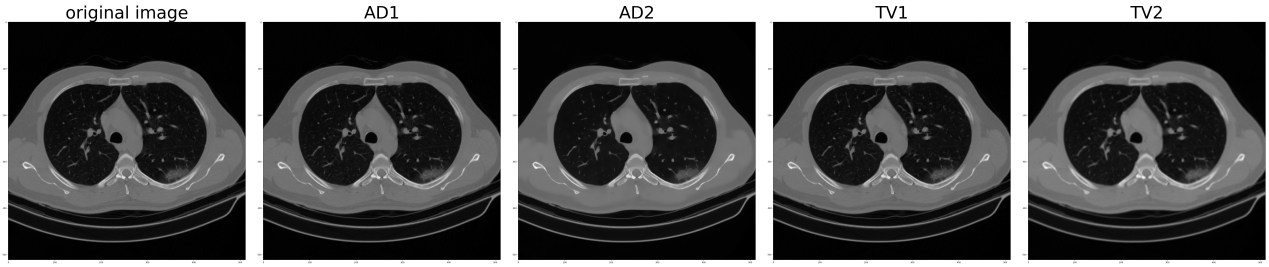

(a) Original and denoised CT

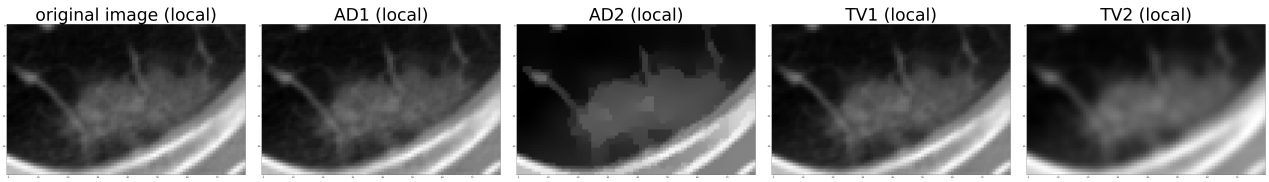

(b) Original and denoised CT (ROI)

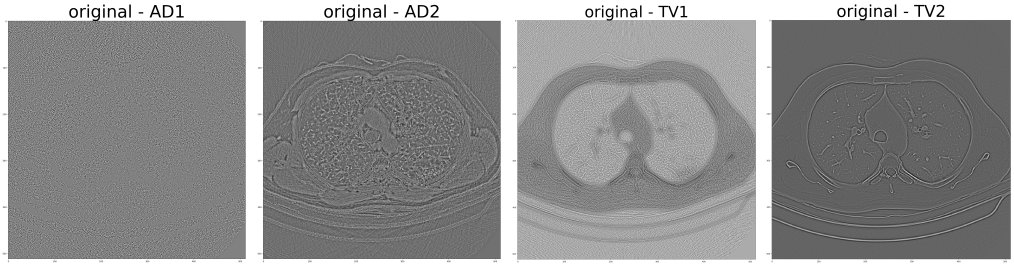

(c) Difference between original and denoised CT

Fig. 3. Example of an original CT image and four types of denoised CT images (from left to right: oriCT, AD1, AD2, TV1, and TV2).

Apart from this visual example, we also conducted mathematical analyses on these four denoised datasets, as shown in Tables II and III, where the mean value and standard deviation of every metrics are presented. From Table II, we can notice that the either the mean pixel value, which reflects the luminance level of an image, or the standard deviation, referring to the variation of pixel values, do not show significant difference between oriCT and the four types of denoised images. Meanwhile, the entropy of all denoised images is higher than oriCT, which comes from the subtraction of noise, a rather homogeneous component in images.

Table III demonstrated the impact of different denoising levels on image quality, from the perspective of traditional IQA metrics. In terms of mean squared error (MSE), AD1 images are the ones closest to oriCTs, while TV2 are the further ones, as well as in terms of peak signal noise ratio (PSNR). Consequently, if we evaluate the quality of denoised CT images by their mathematical indices, TV2 ones are the worst.

TABLE II
INTRA-IMAGE MATHEMATICAL ANALYSIS

Image	Mean (std)	SD (std)	Entropy (std)
oriCT	497.45(89.12)	458.84(16.54)	9.196(0.217)
AD1	497.45(89.12)	458.80(16.54)	17.70(0.115)
AD2	497.45(89.12)	457.61(16.65)	17.96(0.022)
TV1	500.98(89.75)	461.59(16.68)	17.92(0.152)
TV2	500.98(89.75)	455.35(16.77)	17.92(0.146)

TABLE III
INTER-IMAGE MATHEMATICAL ANALYSIS

Image	MSE (std)	PSNR (std)
AD1 vs oriCT	11.546(1.475)	85.743(0.580)
AD2 vs oriCT	654.78(108.20)	68.225(0.694)
TV1 vs oriCT	48.363(8.172)	79.546(0.738)
TV2 vs oriCT	1140.36(257.14)	65.884(1.086)

B. COVID Classifier Performance

Figure 4 illustrates the performance of our COVID classifier on all those five datasets (i.e., oriCT, AD1, AD2, TV1, and TV2), from which we can observe that the models learned from images with lighter denoising weights (i.e., AD1, and TV1) learnt faster than other ones. However their performance is less stable. On the contrary, the models based on AD2 and TV2 images, that is to say the more denoised ones, learnt slightly slower but were more stable. In terms of accuracy, all five models reached an accuracy greater than 0.97 at the end of the training. The lower denoising weight ones (AD1, TV1) achieved a loss (around 0.03) slightly smaller than that of greater denoising weight ones (around 0.08).

To test these trained models, we selected 100 COVID slices and 100 non-COVID slices from the original COVID-CT-MD

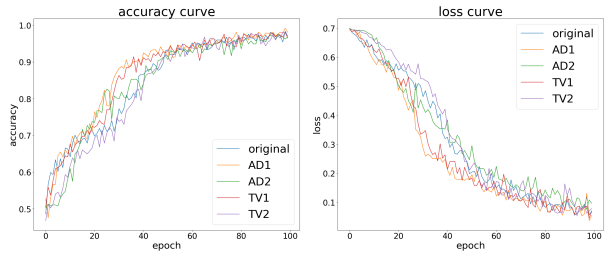

(a) Training accuracy and loss

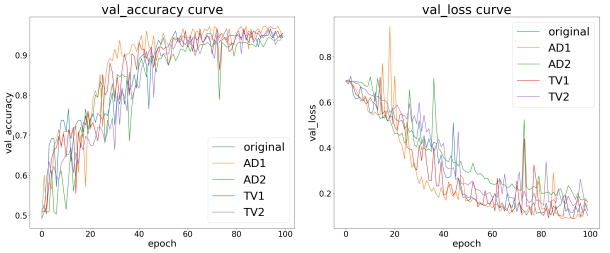

(b) Validation accuracy and loss

Fig. 4. Performance of COVID classifiers on five datasets during training process

database, which were not used for training nor validation. The results are presented in Table IV. The first four columns directly depict the predictions of these models, by giving their true positive (TP), false negative (FN), true negative (TN), and false positive (FP) rates. The last three columns illustrate the sensitivity (Se), specificity (Sp), and area under the ROC curve (AUC). The first part of this table presents the test results of all five models on their corresponding original or denoised images, and the second part shows the results of the four denoised models on the original CT images.

TABLE IV
CLASSIFICATION PERFORMANCE OF DIFFERENT MODELS

Model	TP	FN	TN	FP	Se	Sp	AUC
oriCT	95	5	92	8	0.95	0.92	0.935
AD1	100	0	83	17	1.0	0.83	0.915
AD2	91	9	88	12	0.91	0.88	0.895
TV1	100	0	89	11	1.0	0.89	0.945
TV2	95	5	95	5	0.95	0.95	0.95
AD1 on oriCT	100	0	81	19	1.0	0.81	0.905
AD2 on oriCT	100	0	12	88	1.0	0.12	0.56
TV1 on oriCT	100	0	83	17	1.0	0.83	0.915
TV2 on oriCT	100	0	1	99	1.0	0.01	0.505

We can see that the classification performance of the AD models are worse than the baseline model, while the TV models show a better performance. By comparing the different denoising levels, we can notice that lower denoising weight models (i.e., AD1 and TV1) are indeed less ideal than the corresponding higher denoising weight ones i.e., AD2 and TV2), in spite of their better IQA metrics.

It can also be highlighted that the classification performance of AD2 and TV2 models drastically dropped when evaluated on the original CT images, while that of AD1 and TV1 showed only a slight decrease. This phenomenon might relate to the loss of details (even change of texture) when the denoising weight is great, so that the models trained on denoised images cannot recognize the original ones the same way as they do for denoised ones and therefore failed to classify.

IV. Discussion

From this experiment, three interesting observations can be made: 1) the training process of our COVID classifier is faster on slightly denoised images than on original and heavily denoised ones, 2) models trained on heavily denoised images have better classification performance than those trained on slightly denoised ones, even though the latter obtained better IQA metrics; however, they are not applicable for original images, and 3) TV filtering as a denoising method permits better classification performance than AD filtering and original images.

These discoveries could help us, among others, to better understand the quality of medical images, and to improve classification performance of DL models. For instance, light denoised images could be used as data augmentation, in order to accelerate the training process, while not harming the final classification performance. We could also apply TV filtering with great denoising weight on the whole dataset to achieve better classification results. However, these phenomenons still need further validations since our study is only a preliminary work.

V. Conclusion

In this paper, we presented a study on the influence of two denoising methods, i.e., the anisotropic diffusion (AD) and total variation (TV) filters, at two different levels, on chest CT images for the classification task of COVID-19. A simple but efficient COVID classifier was developed as a model observer for our objective task-based quality assessment.

The classification performance of models trained on four types of denoised images and the original ones demonstrated that the TV filter outperformed the AD filter and original images, and that the heavier denoising weight lead to better classification, in spite of its less favorable image quality metrics and slower training process. On the contrary, lighter denoising weights make training process faster but less helpful for the improvement of the classification performance.

References

[1] Ebrahim Abbasi-Oshaghi, Fatemeh Mirzaei, Farhad Farahani, Iraj Khodadadi, and Heidar Tayebinia, "Diagnosis and treatment of coronavirus disease 2019 (COVID-19): Laboratory, PCR, and chest CT imaging findings," *International Journal of Surgery*, vol. 79, pp. 143–153, 2020.

[2] Arash Mohammadi, Yingxu Wang, Nastaran Enshaei, Parnian Afshar, Farnoosh Naderkhani, Anastasia Oikonomou, Javad Rafiee, Helder Rodrigues de Oliveira, Svetlana Yanushkevich, and Konstantinos Plataniotis, "Diagnosis/prognosis of COVID-19 chest images via machine learning and hypersignal processing: Challenges, opportunities, and applications," *IEEE Signal Processing Magazine*, vol. 38, no. 5, pp. 37–66, 2021.

[3] N. Islam, S. Ebrahimzadeh, J. Salameh, S. Kazi, N. Fabiano, L. Treanor, M. Absi, Z. Hallgrimson, M. Leeflang, L. Hooft, C. van der Pol, R. Prager, S. Hare, C. Dennie, R. Spijker, J. Deeks, J. Dinnes, K. Jenniskens, D. Korevaar, J. Cohen, A. Van den Bruel, Y. Takwoingi, J. van de Wijgert, J. Damen, J. Wang, and M. McInnes, "Thoracic imaging tests for the diagnosis of COVID-19," *Cochrane Database of Systematic Reviews*, vol. 3, 2021.

[4] Yicheng Fang, Huangqi Zhang, Jicheng Xie, Minjie Lin, Lingjun Ying, Peipei Pang, and Wenbin Ji, "Sensitivity of chest CT for COVID-19: comparison to RT-PCR," *Radiology*, vol. 296, no. 2, pp. E115–E117, 2020.

[5] P. Shrimpton and B. Wall, "The increasing importance of X-ray computed tomography as a source of medical exposure," *Radiation Protection Dosimetry*, vol. 57, no. 1-4, pp. 413–415, 1995.

[6] Hantao Liu, Zhou Wang, and R Narayan, "Perceptual quality assessment of medical images," in *Encyclopedia of Biomedical Engineering*, pp. 588–596. Elsevier Amsterdam, The Netherlands, 2019.

[7] Manoj Diwakar and Manoj Kumar, "A review on CT image noise and its denoising," *Biomedical Signal Processing and Control*, vol. 42, pp. 73–88, 2018.

[8] Niranjan Damera-Venkata, Thomas D Kite, Wilson S Geisler, Brian L Evans, and Alan C Bovik, "Image quality assessment based on a degradation model," *IEEE transactions on image processing*, vol. 9, no. 4, pp. 636–650, 2000.

[9] Zhou Wang, Alan C Bovik, Hamid R Sheikh, and Eero P Simoncelli, "Image quality assessment: from error visibility to structural similarity," *IEEE transactions on image processing*, vol. 13, no. 4, pp. 600–612, 2004.

[10] Harrison H Barrett, Jie Yao, Jannick P Rolland, and Kyle J Myers, "Model observers for assessment of image quality," *Proceedings of the National Academy of Sciences*, vol. 90, no. 21, pp. 9758–9765, 1993.

[11] R. Rodrigues, L. Lévêque, J. Gutiérrez, H. Jebbari, M. Outtas, L. Zhang, A. Chetouani, S. Al-Juboori, M. Martini, and A. Pinheiro, "Objective quality assessment of medical image and video: Review and challenges," *arXiv:2212.07396*, 2022.

[12] Lu Zhang-Ge, *Numerical observers for the objective quality assessment of medical images*, Ph.D. thesis, University of Angers, France, 2012.

[13] Xin He and Subok Park, "Model observers in medical imaging research," *Theranostics*, vol. 3, no. 10, pp. 774, 2013.

[14] Zili Liu, David C Knill, and Daniel Kersten, "Object classification for human and ideal observers," *Vision research*, vol. 35, no. 4, pp. 549–568, 1995.

[15] Kyle J. Myers and Harrison H. Barrett, "Addition of a channel mechanism to the ideal-observer model," *J. Opt. Soc. Am. A*, vol. 4, no. 12, pp. 2447–2457, Dec 1987.

[16] Francesc Massanes and Jovan G Brankov, "Evaluation of CNN as anthropomorphic model observer," in *Medical Imaging 2017: Image Perception, Observer Performance, and Technology Assessment*. SPIE, 2017, vol. 10136, pp. 188–194.

[17] Felix Kopp, Marco Catalano, Daniela Pfeiffer, Alexander Fingerle, Ernst Rummeny, and Peter Noël, "CNN as model observer in a liver lesion detection task for X-ray computed tomography: A phantom study," *Medical physics*, vol. 45, no. 10, pp. 4439–4447, 2018.

[18] Weimin Zhou, Hua Li, and Mark A Anastasio, "Approximating the ideal observer and hotelling observer for binary signal detection tasks by use of supervised learning methods," *IEEE transactions on medical imaging*, vol. 38, no. 10, pp. 2456–2468, 2019.

[19] Sameera Mohd Sagheer and Sudhish N George, "A review on medical image denoising algorithms," *Biomedical signal processing and control*, vol. 61, pp. 102036, 2020.

[20] Xin Yi and Paul Babyn, "Sharpness-aware low-dose CT denoising using conditional generative adversarial network," *Journal of Digital Imaging*, vol. 31, no. 5, pp. 655–669, 2018.

[21] Shengkai Zhuo, Zhi Jin, Wenbin Zou, and Xia Li, "RIDnet: Recursive information distillation network for color image denoising," in *Proceedings of the IEEE/CVF International Conference on Computer Vision Workshops*, 2019.

[22] Qingsong Yang, Pingkun Yan, Yanbo Zhang, Hengyong Yu, Yongyi Shi, Xuanqin Mou, Mannudeep Kalra, Yi Zhang, Ling Sun, and Ge Wang, "Low-dose CT image denoising using a generative adversarial network with Wasserstein distance and perceptual loss," *IEEE transactions on medical imaging*, vol. 37, no. 6, pp. 1348–1357, 2018.

[23] Kaiyan Li, Weimin Zhou, Hua Li, and Mark A Anastasio, "Assessing the impact of deep neural network-based image denoising on binary signal detection tasks," *IEEE transactions on medical imaging*, vol. 40, no. 9, pp. 2295–2305, 2021.

[24] Lucie Lévêque, Meriem Outtas, Hantao Liu, and Lu Zhang, "Comparative study of the methodologies used for subjective medical image quality assessment," *Physics in Medicine & Biology*, vol. 66, no. 15, pp. 15TR02, 2021.

[25] Parnian Afshar, Shahin Heidarian, Nastaran Enshaei, Farnoosh Naderkhani, Rafiee Moezedin Javad, Anastasia Oikonomou, Faranak Babaki Fard, Kaveh Samimi, Konstantinos Plataniotis, and Arash Mohammadi, "COVID-CT-MD, COVID-19 computed tomography scan dataset applicable in machine learning and deep learning," *Scientific Data*, vol. 8, 04 2021.

[26] Aijaz Ahmad Reshi, Furqan Rustam, Arif Mehmood, Abdulaziz Alhossan, Ziyad Alrabiah, Ajaz Ahmad, Hessa Alsuwailem, and Gyu Sang Choi, "An efficient cnn model for covid-19 disease detection based on x-ray image classification," *Complexity*, vol. 2021, pp. 1–12, 2021.

[27] Tuan D Pham, "A comprehensive study on classification of covid-19 on computed tomography with pretrained convolutional neural networks," *Scientific reports*, vol. 10, no. 1, pp. 1–8, 2020.

[28] Asmaa Abbas, Mohammed M Abdelsamea, and Mohamed Medhat Gaber, "Classification of covid-19 in chest x-ray images using detrac deep convolutional neural network," *Applied Intelligence*, vol. 51, pp. 854–864, 2021.

[29] Mucahid Barstugan, Umut Ozkaya, and Saban Ozturk, "Coronavirus (covid-19) classification using ct images by machine learning methods," *arXiv preprint arXiv:2003.09424*, 2020.

[30] Osama R Shahin, Hamoud H Alshammari, Ahmed I Taloba, and Rasha M Abd El-Aziz, "Machine learning approach for autonomous detection and classification of covid-19 virus," *Computers and Electrical Engineering*, vol. 101, pp. 108055, 2022.

[31] Sara Hosseinzadeh Kassania, Peyman Hosseinzadeh Kassanib, Michal J Wesolowskic, Kevin A Schneidera, and Ralph Detersa, "Automatic detection of coronavirus disease (covid-19) in x-ray and ct images: a machine learning based approach," *Biocybernetics and Biomedical Engineering*, vol. 41, no. 3, pp. 867–879, 2021.

[32] Shahin Heidarian, Parnian Afshar, Nastaran Enshaei, Farnoosh Naderkhani, Moezedin Javad Rafiee, Faranak Babaki Fard, Kaveh Samimi, Farokh Atashzar, Anastasia Oikonomou, Konstantinos Plataniotis, and Arash Mohammadi, "COVID-FACT: A fully-automated capsule network-based framework for identification of COVID-19 cases from chest CT scans," *Frontiers in Artificial Intelligence*, vol. 4, 2021.

[33] Joachim Weickert, *Anisotropic diffusion in image processing*, vol. 1, Teubner Stuttgart, 1998.

[34] David Moroni Strong, *Adaptive total variation minimizing image restoration*, University of California, Los Angeles, 1997.

[35] Pietro Perona and Jitendra Malik, "Scale-space and edge detection using anisotropic diffusion," *IEEE Transactions on pattern analysis and machine intelligence*, vol. 12, no. 7, pp. 629–639, 1990.

[36] Leonid I Rudin, Stanley Osher, and Emad Fatemi, "Nonlinear total variation based noise removal algorithms," *Physica D: nonlinear phenomena*, vol. 60, no. 1-4, pp. 259–268, 1992.